

## Evidence for the involvement of FXR signaling in ovarian granulosa cell function

Kentaro TAKAE<sup>1)</sup>, Mizuho NAKATA<sup>1)</sup>, Takafumi WATANABE<sup>2)</sup>, Hiroshi SASADA<sup>3)</sup>, Hiroshi FUJII<sup>4, 5)</sup> and Ikuo TOMIOKA<sup>1, 5)</sup>

<sup>1)</sup>Laboratory of Applied Reproductive Science, Faculty of Agriculture, Shinshu University, Nagano 399-4598, Japan

<sup>2)</sup>Laboratory of Animal Functional Anatomy, Faculty of Agriculture, Shinshu University, Nagano 399-4598, Japan

<sup>3)</sup>Laboratory of Animal Reproduction, School of Veterinary Medicine, Kitasato University, Aomori 034-8628, Japan

<sup>4)</sup>Laboratory of Biochemistry, Faculty of Agriculture, Shinshu University, Nagano 399-4598, Japan

<sup>5)</sup>Department of Interdisciplinary Genome Sciences and Cell Metabolism, Institute for Biomedical Sciences, Interdisciplinary Cluster for Cutting Edge Research, Shinshu University, Nagano 399-4598, Japan

**Abstract.** Farnesoid X receptor (FXR) is mainly present in enterohepatic tissues and regulates cholesterol, lipid, and glucose homeostasis in coordination with target genes such as *SHP* and *FABP6*. Although FXR has been revealed to be expressed in reproductive tissues, FXR function and expression levels in the ovary remain unknown. In this study, we investigated FXR expression in mouse ovaries and its target genes in ovarian granulosa cells. *In situ* hybridization and immunohistochemical staining showed that FXR was mainly distributed in secondary and tertiary follicles. The agonist-induced activation of FXR in cultured granulosa cells induced the expression of *SHP* and *FABP6*, while siRNA targeting of *FXR* decreased *CYP19a1* and *HSD17b1* expression. Upon examination of the roles of *SHP* and *FABP6* in granulosa cells, we found that *SHP* overexpression significantly decreased *StAR*, *CYP11a1*, and *HSD3b* gene expression. In addition, siRNA targeting of *FABP6* decreased *CYP19a1* and *HSD17b1* expression, while *FABP6* overexpression increased *CYP19a1* expression. In conclusion, the present study demonstrates the presence of FXR signaling in the ovary and reveals that FXR signaling may have a role in function of granulosa cells.

**Key words:** Farnesoid X receptor (FXR), Granulosa cell, Ovary, Steroidogenesis

(J. Reprod. Dev. 65: 47–55, 2019)

**E**fficient production of eggs is important for the production of offspring, not only in agricultural industries, but also for the preservation of endangered animals. In the ovary, eggs are yielded as an output of oocyte growth through follicular growth and development. During follicular development, the interaction between an oocyte and the granulosa cells is crucial for normal oocyte growth. Many factors for oocyte growth are produced and regulated via the autocrine and/or paracrine pathways [1]. Various kinds of bile acids have been recently detected in human and bovine follicular fluid [2, 3], and the concentrations were 2-fold higher in follicular fluids than those in serum. Moreover, lactating cows have a 3-fold higher concentration of total bile acids in both follicular fluid and plasma, than that in heifers [4], and several enzymes in the bile acid biosynthesis pathway are present in both granulosa cells and oocytes [5].

Originally, the synthesis of bile acids was shown to be regulated in the liver by FXR. Bile acids serve as natural ligands for FXR, and activated FXR subsequently activates the transcription of several target

genes, such as *SHP* (small heterodimer partner) and *FABP6* (fatty acid-binding protein 6). *SHP* binds to and represses the transcriptional activities of LHR-1 (liver receptor homolog 1), which induces *Cyp7a1* (cytochrome P450 7A1) expression, a liver-specific cholesterol 7 $\alpha$ -hydroxylase [6], causing a reduction in bile acid synthesis [7, 8]. *FABP6*, an intracellular protein expressed in the distal ileum, plays a role in transcellular shuttling of bile acids [9–14]. Bile acid-FXR signaling and its target genes represent major regulatory factors for bile acid metabolism in enterohepatic tissues.

Recent studies have revealed the existence of FXR in non-enterohepatic tissues, such as bone marrow [15, 16], brain neurons [17], cardiomyocytes [18], blood vessels [19], and male reproductive tissues [20–22]. In the testis, the activation of FXR by bile acids affects steroidogenesis, which significantly decreases the production of sex steroids in porcine Leydig cells [23]. In addition, FXR competitively binds to the steroidogenic factor 1 response element, which regulates aromatase expression in tumor Leydig cells [21]. Although evidence for bile acid-FXR signaling in males has been established, information on this signaling in females is limited.

To investigate the role of FXR in the ovary, we examined its expression, with a focus on the follicles, and the potential activity of FXR signaling in granulosa cells. To our knowledge, this is the first study that shows the evidence for the involvement of FXR signaling in the function of ovarian granulosa cells.

Received: April 12, 2018

Accepted: November 1, 2018

Published online in J-STAGE: November 16, 2018

©2019 by the Society for Reproduction and Development

Correspondence: I Tomioka (e-mail: tomioka@shinshu-u.ac.jp)

This is an open-access article distributed under the terms of the Creative Commons Attribution Non-Commercial No Derivatives (by-nc-nd) License. (CC-BY-NC-ND 4.0: <https://creativecommons.org/licenses/by-nc-nd/4.0/>)

## Materials and Methods

### Animals

All experiments were conducted in accordance with the institutional guidelines established by Shinshu University for the care and use of laboratory animals, and approved by the ethics committee for animal research of Shinshu University, Japan. ICR mice were purchased from Japan SLC (Shizuoka, Japan) and housed in a temperature-controlled room under a 12-h/12-h light-dark cycle.

### Production of ovary specimens

Adult female mice at the age of 10–12 weeks were euthanized by cervical dislocation, and the ovaries were collected and fixed in 4% paraformaldehyde in phosphate-buffered saline solution (PBS) for 24 h, followed by embedding in paraffin. Five-micrometer-thick sections were prepared from each ovary, mounted on silane-coated glass slides, and analyzed.

### In situ hybridization

To determine the localization of *FXR* mRNA in the ovaries, *in situ* hybridization using an antisense oligonucleotide probe labeled at the 5' end with digoxigenin (DIG), was performed as previously described [24]. Briefly, the glass slides containing ovary sections were placed on a warm plate and dried overnight at 39°C. The next day, specimens were dewaxed in four xylene baths for 5 min each, and rehydrated in a descending alcohol series using distilled water. The slides were then immersed in PBS. The sequence of the *FXR* antisense probe was 5'-CAGAGCGTACTCCTCCTGAGTC-3', and the sense probe sequence was 5'-GACTCAGGAGGAGTACGCTCTG-3'. All hybridization, washing, and visualization steps were performed using a commercial kit (IsHyb In Situ Hybridization Kit; Biochain Institute, Newark, CA, USA), according to the manufacturer's instructions. Bound probe was visualized using an alkaline phosphatase-conjugated anti-DIG antibody and a nitroblue tetrazolium/5-bromo-4-chloro-3-indolyl-phosphate solution. The same procedure was performed with a sense oligonucleotide probe, which served as a negative control. After hybridization, the sections were observed using an IX73 inverted microscope and a DP73 microscope digital camera (Olympus, Tokyo, Japan).

### Immunohistochemical staining

For antigen retrieval, the slides were placed in vertical staining jars containing HistoVT One (Nacalai tesque, Tokyo, Japan) and autoclaved at 121°C for 15 min. The jars were cooled at room temperature for 30 min and rinsed with PBS. Endogenous peroxidase activity was blocked by adding 30% hydrogen peroxidase at a 1:100 dilution in methanol for 20 min, after which slides were washed in PBS three times. To reduce non-specific staining, the slides were incubated in PBS containing 10% Blocking One Histo (Nacalai tesque), and then washed with PBS. For detection of *FXR*, the slides were incubated with rabbit anti-*FXR* IgG (H-130, Lot No. A2315, Santa Cruz Biotechnology, Santa Cruz, CA, USA) diluted with PBS (1:300) overnight in a humidified chamber at 4°C. The slides were then incubated with horseradish peroxidase-conjugated donkey anti-rabbit IgG (Biolegend, San Diego, CA, USA) diluted with PBS (1:1000) at room temperature for 3 h and then washed

three times in PBS. The color was developed with a freshly prepared solution of 3,3'-diaminobenzidine (DAB) Peroxidase Stain DAB Kit (brown stain) (Nacalai tesque), and the sections were dehydrated and mounted. In the negative control, the sections were incubated with PBS instead of the specific primary antibody.

### Collection and culture of granulosa cells

Immature mice at the age of 3 weeks were intraperitoneally injected with 5 IU of pregnant mare serum gonadotropin (PMSG, Aska Animal Health, Tokyo, Japan) followed by 5 IU of human chorionic gonadotropin (hCG, Aska Animal Health, Tokyo, Japan) 48 h later. At 0, 24, 48, and 60 h after PMSG injection, mice were euthanized by cervical dislocation, and granulosa cells were collected from ovarian follicles by puncturing them using a 26G needle and subjected to further analysis. In experiments for cell culture, granulosa cells collected at 24 h after PMSG injection were washed twice in PBS before culturing. The cells were placed onto a gelatin-coated dish and cultured in DMEM containing 1% fetal bovine serum (Sigma-Aldrich Japan, Tokyo, Japan) and 1% Insulin-Transferrin-Selenium mixture (ITS-G, Wako, Tokyo, Japan). Four to six days after culture, the confluent cells were passaged in a 12-well plate dish, and subjected to the experiments for ligand supplementation and gene knockdown. In ligand supplementation experiments, the cells were cultured for 24 h in either a medium supplemented with 50  $\mu$ M chenodeoxycholic acid (CDCA, Nacalai tesque) as a natural ligand for *FXR*, 1  $\mu$ M GW4064 (AdooQ BioScience, Irvine, CA, USA) as an agonist of *FXR*, or 10  $\mu$ M Z-guggulsterone (Sigma) as an antagonist of *FXR*, and then subjected to further analysis.

### SiRNA knockdown of *FXR*, *SHP*, and *FABP6*

The cultured granulosa cells were transfected with either of 15 nM negative control siRNA (universal negative control siRNA, Nippongene, Tokyo, Japan), *FXR* siRNA (5'-uguucuguuagcauacuuTT-3', Nippongene), *SHP* siRNA (5'-uccugugcaggugugcgaTT-3', Nippongene), or *FABP6* siRNA (5'-uuguucaugacacacagaTT-3', Nippongene) using Lipofectamine RNAi-MAX (Thermo Fisher Scientific, Waltham, MA, USA) according to the manufacturers' instructions. After treatment with siRNA, granulosa cells were cultured in a medium with or without GW for 24 h.

### Construction of the *SHP* and *FABP6* overexpression vectors and lentiviral vector preparation

Mouse *SHP* (NM\_011850.3) and *FABP6* (NM\_008375.2) were cloned from the mRNA of granulosa cells. A marker gene encoding Venus protein was linked by an internal ribosomal entry site (IRES), and the resultant constructs were inserted into a self-inactivating lentiviral vector carrying the CMV promoter (RIKEN, Tsukuba, Japan). Lentiviral vectors were produced as previously described [3]. Briefly, lentiviruses were generated by co-transfection of lentiviral vectors coding for CMV-SHP-IRES-Venus or CMV-FABP6-IRES-Venus, pCAG-HIVgp (RIKEN), and pCMV-VSV-G (RIKEN), into 293FT packaging cells (Invitrogen, Thermo Fisher Scientific). The medium containing viral particles was spun at 50,000  $\times$  g for 2 h at 4°C, and the viral pellet was resuspended in 1/100 of the volume of the original lentiviral vector supernatant. The granulosa cells collected were seeded at  $1 \times 10^5$  cells per well in a 12-well plate

dish one day before transduction. After replacing the medium with virus-containing supernatant supplemented with 4  $\mu\text{g/ml}$  polybrene (Nacalai tesque), the cells were incubated for 12 h.

#### RNA extraction and reverse transcription (RT)

RNA was isolated from granulosa cells using the NucleoSpin RNA mini kit (Takara, Tokyo, Japan) according to the manufacturer's instructions. First-strand cDNA was synthesized from RNA using the ReverTra Ace qPCR RT Master Mix with gDNA Remover (TOYOBO, Tokyo, Japan). As a negative control, RNA was allowed to react with the cDNA synthesis reaction mixture in the absence of reverse transcriptase.

#### PCR analysis

We used a panel of specific primers to detect the expression of each of the four *FXR* isoforms:  $\alpha$ -Fwd and 1-Rev for *FXR $\alpha$ 1*,  $\alpha$ -Fwd and 2-Rev for *FXR $\alpha$ 2*,  $\beta$ -Fwd and 1-Rev for *FXR $\beta$ 1*, and  $\beta$ -Fwd and 2-Rev for *FXR $\beta$ 2* (Table 1). The cDNAs were subjected to PCR for 40 cycles of 98°C for 10 sec, 64°C for 30 sec, and 72°C for 30 sec using EmeraldAmp PCR Master Mix (Takara, Tokyo, Japan) according to the manufacturer's instructions. PCR products were electrophoresed on a 1% agarose gel at 100 V for 35 min.

#### Real-time PCR analysis

To quantify the relative expression of total *FXR*, ex8-Fwd and ex9-Rev primers were used (Table 1). To detect *GAPDH* expression, *GAPDH*-Fwd and *GAPDH*-Rev primers were used (Table 1). The cDNAs were subjected to real-time PCR for 45 cycles of 98°C for 10 sec, 60°C for 15 sec, and 72°C for 15 sec using Ti-SYBR Green (Takara) and a LightCycler Nano (Roche, Basel, Switzerland) according to the manufacturer's instructions. All real-time PCR results were normalized with the expression of *GAPDH*, and the relative transgene expression levels were shown as the mean  $\pm$  standard errors (SE) of at least three repeats in each experimental group.

#### Statistical analysis

Statistical analysis was performed using a Dunnett's multiple comparison test with a significance of  $P < 0.05$ .

## Results

#### Distribution of *FXR* in the ovary

To examine the presence of *FXR* in the ovary, we performed *in situ* hybridization of *FXR* mRNA (Fig. 1A–C) and immunohistochemical staining for the *FXR* protein (Fig. 1D–F) in ovarian sections of adult mice. Both analyses showed that *FXR* was mostly distributed in secondary and tertiary follicles, particularly within granulosa cells, but not in the regressive corpus luteum and corpus albicans. From these results, we focused on granulosa cells in the following experiments.

#### Expression of *FXR* isoforms and time dependent gene expression of *FXR* in granulosa cells

Four isoforms of *FXR* mRNA have been identified (Fig. 2A), with each regulating its own target genes [25]. Therefore, we first identified the *FXR* isoforms that were expressed in granulosa cells. RT-PCR analysis showed that granulosa cells expressed *FXR $\alpha$ 1* and

**Table 1.** Primer sequences used in the present study

| Gene           | Primer name   | Primer sequences                  |
|----------------|---------------|-----------------------------------|
| <i>FXR</i>     | $\alpha$ -Fwd | 5'- ggcccaaagcaatccaaggatc -3'    |
|                | $\beta$ -Fwd  | 5'- ctaaggatggtgatgcagtttc -3'    |
|                | 1-Rev         | 5'- gttacaacacctgtatacatcattc -3' |
|                | 2-Rev         | 5'- ttcagttacaacattcagcc -3'      |
|                | ex8-Fwd       | 5'- gaaactctctgccggtcatgc -3'     |
|                | ex9-Rev       | 5'- cagagcgtactcctctctgagtc -3'   |
| <i>SHP</i>     | Forward       | 5'- gtacctgaaggcagcagtcctc -3'    |
|                | Reverse       | 5'- taccagggctccaagacttcac -3'    |
| <i>FABP6</i>   | Forward       | 5'- gcaagaagtcaaggctaccgtg -3'    |
|                | Reverse       | 5'- acgcgctcataggtcacatcc -3'     |
| <i>STAR</i>    | Forward       | 5'- ccacctgatggtgcttcac -3'       |
|                | Reverse       | 5'- tctcgataggacctggtgatg -3'     |
| <i>CYP19A1</i> | Forward       | 5'- ggtcgaagcagcaatcctcgaag -3'   |
|                | Reverse       | 5'- gcatgaccaagtcacaacagg -3'     |
| <i>HSD3B</i>   | Forward       | 5'- tcattcccagcagaccatcc -3'      |
|                | Reverse       | 5'- ccctgcaacatcaactgagctg -3'    |
| <i>CYP11A1</i> | Forward       | 5'- acctgtgtctctttatagctc -3'     |
|                | Reverse       | 5'- gccatctcataaagggtccactgc -3'  |
| <i>HSD17B1</i> | Forward       | 5'- tatgagcaagcctgagcgag -3'      |
|                | Reverse       | 5'- tcgtggagaagtagecgcag -3'      |
| <i>GAPDH</i>   | Forward       | 5'- ttggcatttggaaggctc -3'        |
|                | Reverse       | 5'- catcacgccacagcttccag -3'      |

*2*, but not *1* and *2*, whereas liver cells expressed *FXR $\alpha$ 2* and *2*, and intestine expressed *FXR $\beta$ 1* and *2* (Fig. 2B). These results showed that *FXR $\alpha$ 1* is specific to granulosa cells, and that these cells strongly expressed *FXR $\alpha$ 2* similar to levels seen in the liver. We next investigated the time-dependent gene expression of *FXR* in ovarian granulosa cells after PMSG treatment. A total *FXR* expression in granulosa cells increased at 24 and 48 h after PMSG treatment by 23.9- and 8.7-fold, compared with that at 0 h, respectively.

#### *FXR* signaling in granulosa cells

To investigate the role of *FXR* signaling in granulosa cells, we examined the expression of the known *FXR* target genes, *SHP* and *FABP6*. We treated granulosa cells with either of natural ligand (CDCA), agonist (GW), or antagonist (Gug) of *FXR*. As a result, *FXR*, *SHP*, and *FABP6* expression were significantly increased by GW treatment, whereas the expression of each gene was decreased after Gug treatment (Fig. 3A–C). After GW treatment, *SHP* and *FABP6* expression were significantly increased at 7.1 and 24.4-fold that of the control, respectively. After CDCA treatment, they were 2.0- and 1.7-fold higher than controls, respectively, although, this was not statistically significant. These results showed a possible involvement of *FXR* signaling in ovarian granulosa cells.

To further confirm that *FXR* mediates GW-induced upregulation of *SHP* and *FABP6*, we transfected granulosa cells with *FXR* siRNA prior to treatment with GW. As shown in Fig. 3E and 3F, knockdown of *FXR* significantly inhibited the increase of *SHP* and *FABP6* expression by GW treatment. As the present experiment showed that *FXR* could activate the expression of its already-known target genes in ovarian

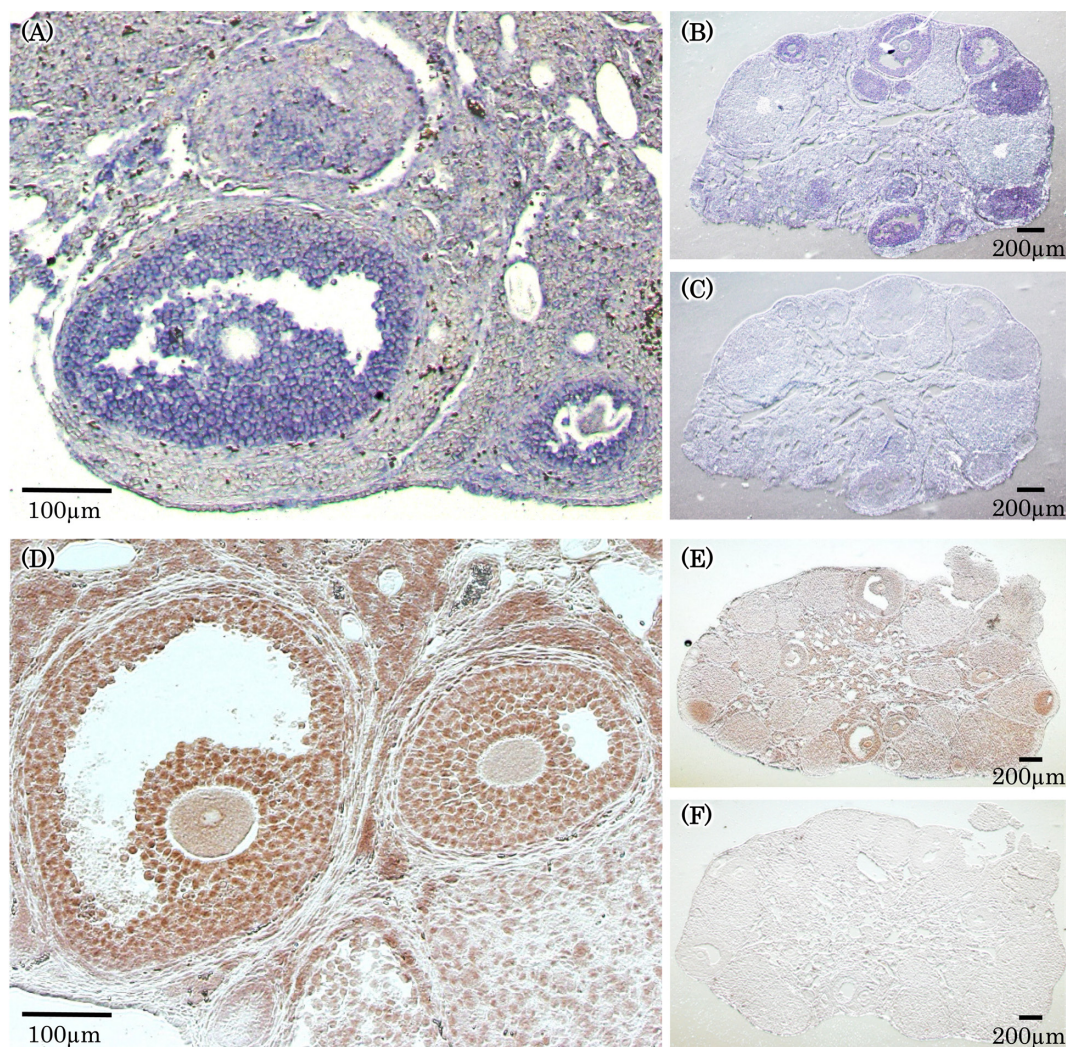


**Fig. 1.** Distribution of FXR in mouse ovaries, detected by *in situ* hybridization (A, B, and C) and immunohistochemical staining (D, E, and F). A and D are enlarged figures from B and E, respectively, and C and F show data from the negative control. FXR was mainly distributed in secondary and tertiary follicles, but not in the regressive corpus luteum or corpus albicans.

granulosa cells, we were interested to know how FXR functions on granulosa cells. We therefore investigated whether FXR has any role in steroid synthesis, as it is known that steroid synthesis is one of the main functions of granulosa cells. As a first step, we analyzed the expression of progesterone synthesis-related genes (*StAR*, *CYP11a1*, and *HSD3b*), and estradiol synthesis-related genes (*CYP19a1* and *HSD17b1*) by quantitative RT-PCR. As shown in Fig. 3G, FXR siRNA transfection had no effect on the expression of progesterone synthesis-related genes, whereas expression of both *CYP19a1* and *HSD17b1* were significantly decreased.

#### *Involvement of the FXR target genes, SHP and FABP6, in steroid synthesis*

From the experiments shown in Fig. 3, it was revealed that FXR has a possible role in the expression of estradiol synthesis genes. As FXR was able to activate expression of both *SHP* and *FABP6* in

granulosa cells, we next sought to investigate the FXR targeted genes that are committed in that cascade. For this, we investigated the direct effects of *SHP* or *FABP6* on progesterone- or estradiol-related gene expression. As shown in Fig. 4A, knockdown of *SHP* had no effect on either progesterone or estradiol synthesis-related gene expression, although *SHP* overexpression significantly inhibited *StAR*, *CYP11a1*, and *HSD3b* gene expression, but without any effect on *HSD17a* or *CYP19a1* gene expression (Fig. 4B). In contrast, as shown in Fig 4C, *FABP6* siRNA transfection only decreased the expression of estradiol-related genes. After *FABP6* overexpression, only *CYP19a1* gene expression was significantly increased (Fig. 4D).

## Discussion

Although recent studies have revealed evidence for the function of FXR in the testis and in male fertility [21, 22], little information on

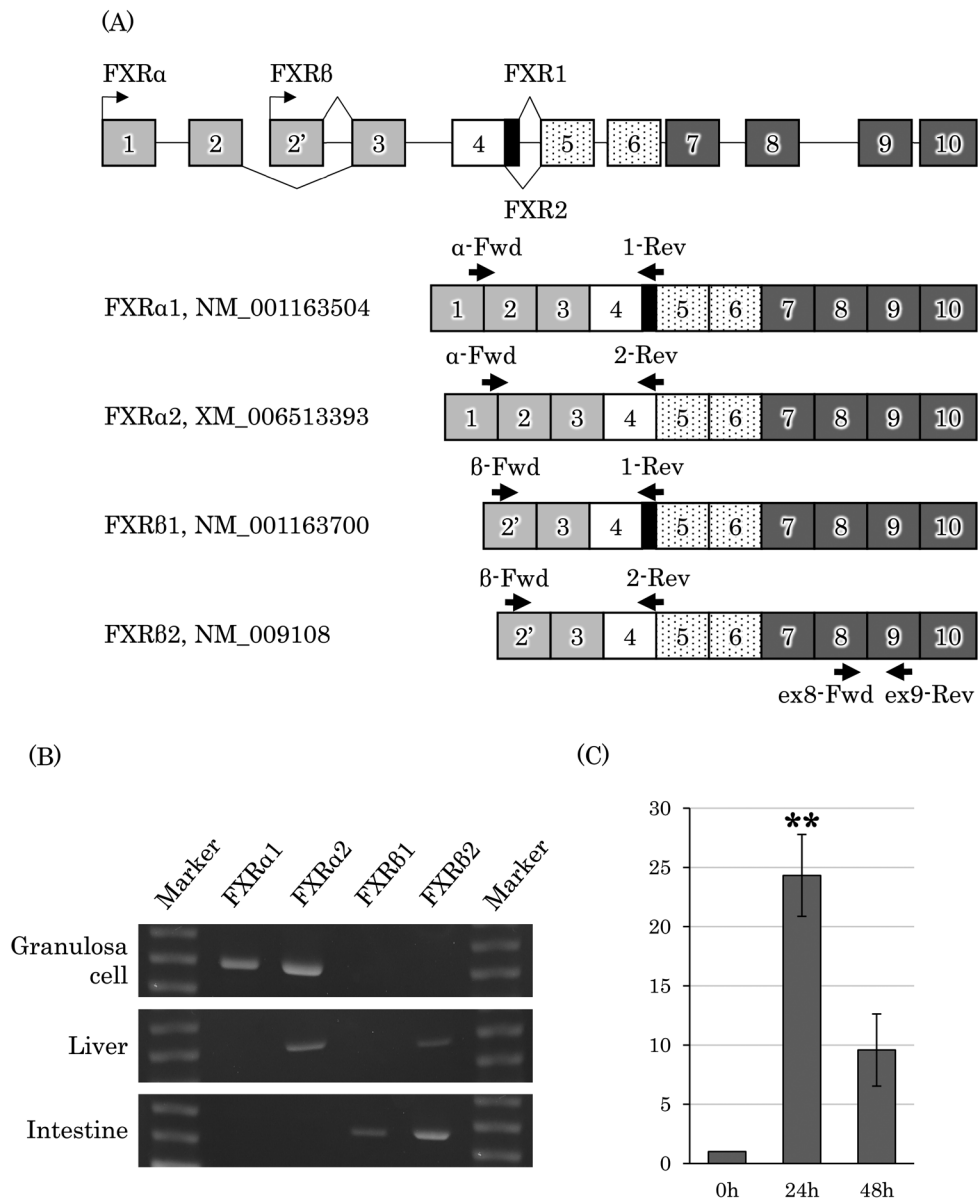


**Fig. 2.** Expression of *FXR* isoforms in ovarian granulosa cells. (A) *FXR* isoforms according to differences in the initial region (exons 1–3) of mRNA ( $\alpha$  and  $\beta$ ) and the presence (1) or absence (2) of a 12-bp insert in exon 4. Exon 1–3: Transactivation-independent domain. Exon 4: DNA-binding domain. Exon 5–6: Hinge region. Exon 7–10: Ligand-binding domain, transactivation-dependent domain. Black: A 12-bp insert. (B) Gene expression of *FXR* isoforms in ovarian granulosa cells, liver, and intestine. (C) Time-dependent gene expression of *FXR* in granulosa cells.

the function of FXR signaling in females has been reported. In the present study, we showed evidence for the existence of FXR signaling in the ovary. *In situ* hybridization and immunohistochemistry both revealed that FXR is distributed mainly in secondary and tertiary follicles, particularly within granulosa cells. In addition, we clarified that the *FXR $\alpha$ 1* and  *$\alpha$ 2* isoforms are expressed in granulosa cells. Since Vaquero *et al.* reported that each isoform regulates its own target genes [25], and that *FXR $\alpha$ 2* is strongly expressed in liver, the present finding suggests the possibility that ovarian FXR may be involved in cholesterol metabolism, as in the liver. Moreover, the present study

showed that *FXR* gene expression increases significantly 24 h after PMSG treatment, and that knockdown of *FXR* significantly decreases estrogen synthesis-related gene expression in ovarian granulosa cells.

*FXR*, originally identified as an orphan nuclear hormone receptor [26], regulates bile acid synthesis, fat metabolism, and glucose homeostasis in enterohepatic tissues. Bile acids bind *FXR* as physiologically relevant ligands, and then the activated *FXR* induces the expression of many target genes. In virgin and pregnant rabbits [20], it was shown by immunostaining that *FXR* is present in ovarian follicles. In addition, recent studies showed the existence of various

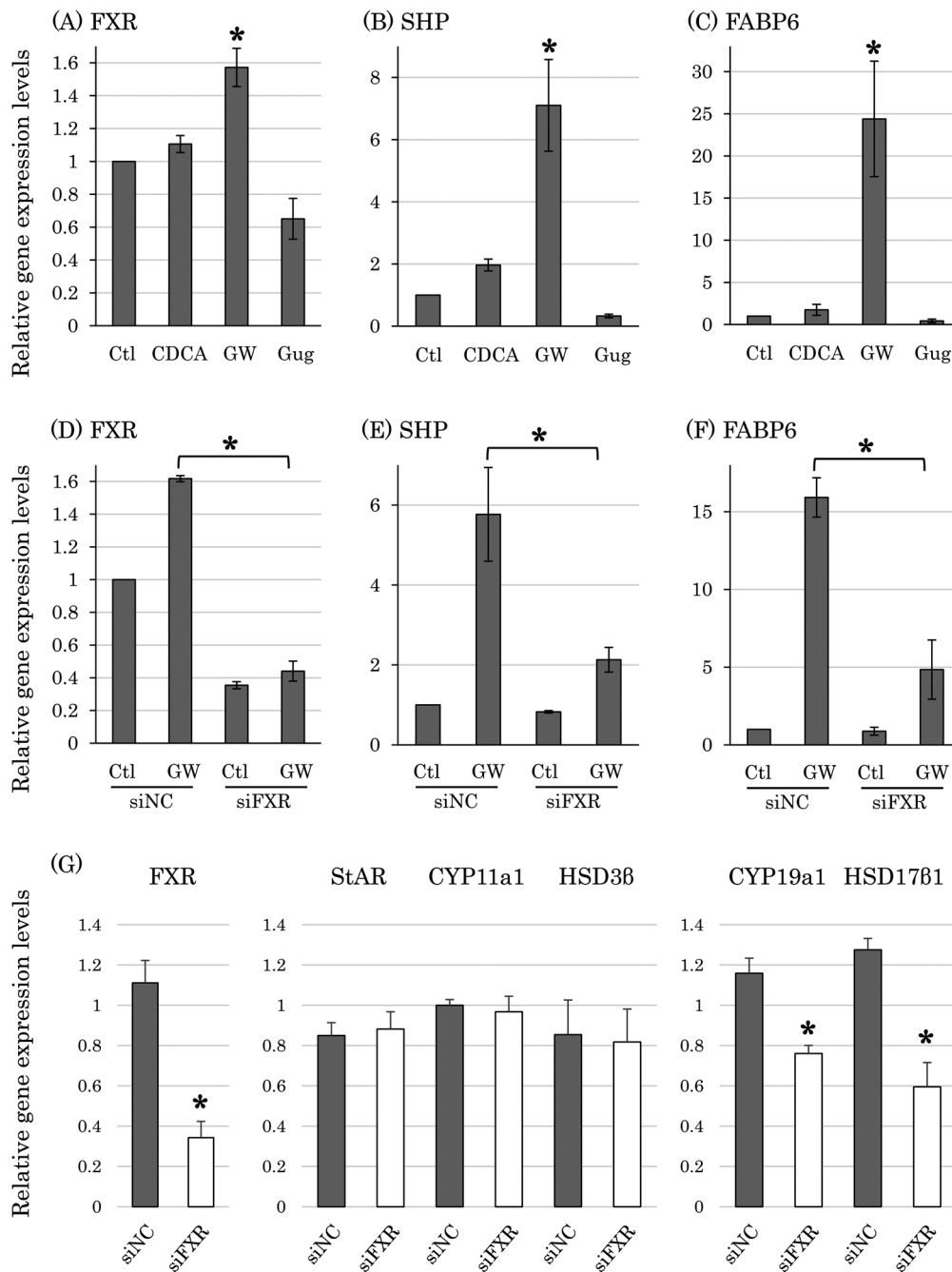


**Fig. 3.** FXR signaling in granulosa cells. (A, B, and C) Relative gene expression levels of *FXR*, *SHP*, and *FABP6* in granulosa cells treated with 50  $\mu$ M CDCA, 1  $\mu$ M GW4064, or 10  $\mu$ M guggulsterone (Gug) for 24 h. \*  $P < 0.05$  compared with the control (Ctl). (D, E, and F) Relative gene expression levels of *FXR*, *SHP*, and *FABP6* in granulosa cells with *FXR* siRNA (siFXR) or negative control siRNA (siNC) treatment, with or without GW4064 for 24 h. \*  $P < 0.05$  between siNC and siFXR in GW treatments. (G) Effect of siRNA targeting of *FXR* on the expression of steroid synthesis-related genes. In each graph, the gene expression level in the Ctl or siNC group is presented as 1. Data are shown as the mean  $\pm$  SE from at least three independent experiments.

kinds of bile acids in follicular fluid, with higher concentrations than those observed in serum [2, 3]. Moreover, several bile acid biosynthesis pathway enzymes are present in both granulosa cells and oocytes [5]. Therefore, together with the present finding that

FXR exists in follicles, particularly within granulosa cells, it seems that bile acid-FXR signaling acts upon the function of granulosa cells. Furthermore, in bovine, follicle size is correlated with the concentration of bile acids and the molecular subspecies are different

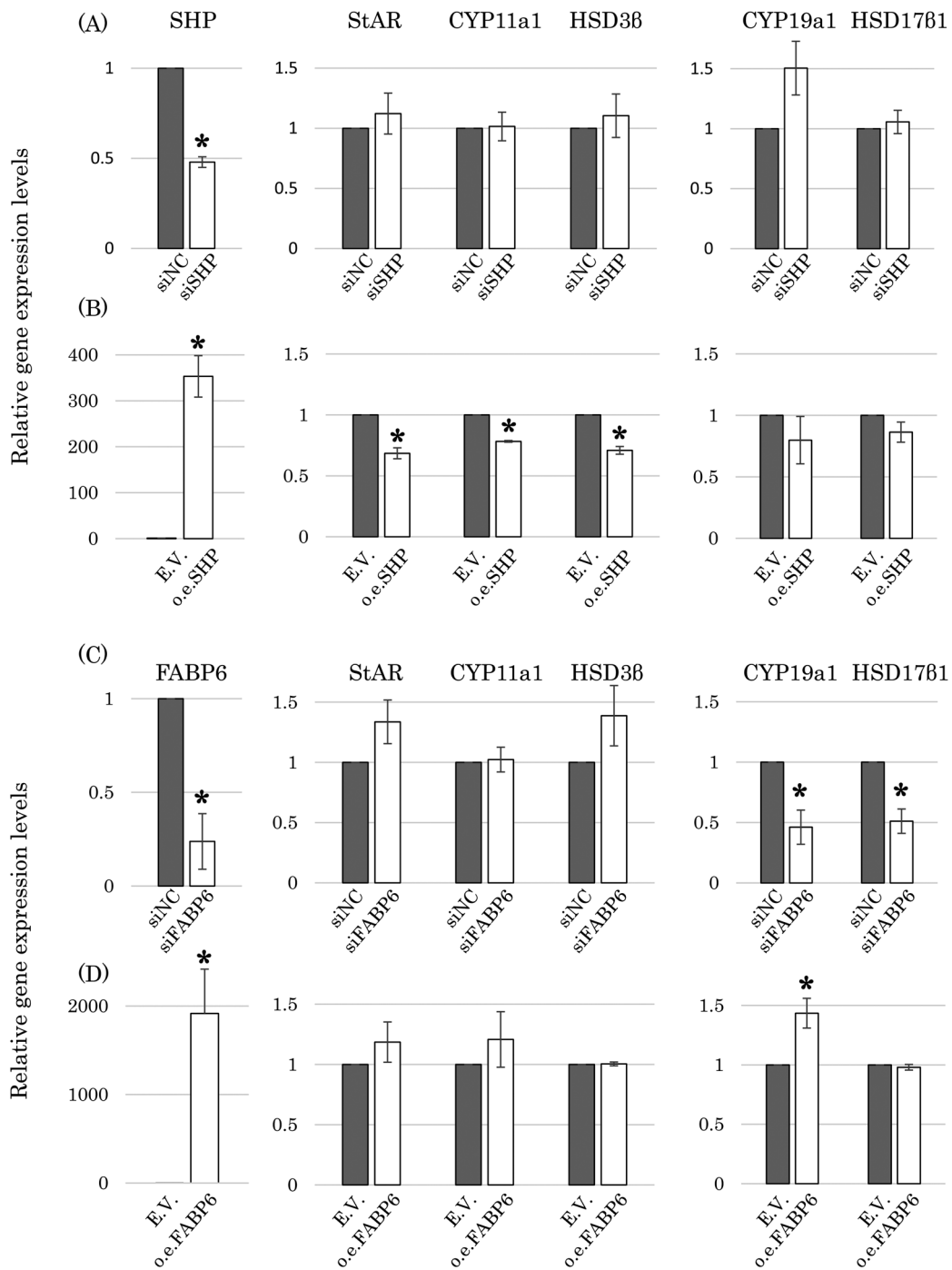


**Fig. 4.** Relationship between SHP or FABP6 and steroid synthesis gene expression. (A) Granulosa cells were transfected with (A) *SHP* siRNA (siSHP), (B) *SHP* overexpression vector (o.e.SHP), (C) *FABP6* siRNA (siFABP6), and (D) *FABP6* overexpression vector (o.e.FABP6), and quantitative RT-PCR was performed for the indicated genes. The gene expression level in the negative control siRNA (siNC) or empty vector-transfected (E.V.) granulosa cells is presented as 1. \*  $P < 0.05$  compared with siNC or E.V. Data are shown as the mean  $\pm$  SE from at least three independent experiments.

between follicles [3], suggesting a relationship between bile acid-FXR signaling and follicle growth. This speculation may be supported by the finding of a positive relationship between the concentration

of bile acids and oocyte quality [2].

In this study, *in vitro* experiments with the natural ligand and agonist showed that in granulosa cells, FXR upregulates *SHP* and

*FABP6* gene expression as it does in enterohepatic tissues, but that the stimulatory levels were different between two drugs. This difference may be related to their optimal concentrations under *in vitro* conditions. In the present study, the concentration of CDCA used was 50  $\mu\text{M}$ . One of the reasons for this may be that FXR in enterohepatic tissues binds to higher concentration of bile acid, and that more than 100  $\mu\text{M}$  of bile acid is generally used in such tissue culture experiments, although bile acid concentration of human follicular fluid is about 10  $\mu\text{M}$  [2], on which the present study was based. Besides bile acid acting as a natural ligand, there are likely to be other, unknown ligands in ovarian granulosa cells, such as sulfated progesterone metabolites [27] and androsterone [28].

It is known that FXR functions mainly via its target genes. When we examined the functions of FXR-targeted genes, knockdown of *FXR* with siRNA suppressed the expression of both *SHP* and *FABP6* by the agonist. In addition, such treatment had less of an effect on the expression of *CYP19a1* and *HSD17b1*, but not of *StAR*, *CYP11a1*, and *HSD3b*. In a further experiment involving direct suppression by siRNA, we found that there was no effect on steroidogenesis-related gene expression, except upon *CYP19a1* and *HSD17b1*. The present findings first showed that on ovarian granulosa cells, FXR functions via its targeted gene. In liver, FXR induces the expression of *SHP*, and *SHP* subsequently binds to and represses the transcriptional activities of LRH-1, inducing *Cyp7a1* gene expression [6], and resulting in the reduction of bile acid synthesis [7, 8]. In granulosa cells, cholesterol is converted to sex hormones by steroidogenic enzymes, whose expression are regulated by LRH-1 [29, 30]. LRH-1 is an essential factor for both ovulation and pregnancy [31, 32], and its transcriptional activity is repressed by *SHP* through direct binding [7, 8]. This suggests that the FXR-*SHP* cascade in granulosa cells downregulates progesterone synthesis-related genes via a repression of LRH-1-dependent transcriptional activity.

Besides the finding that treatment with *FABP6* siRNA suppressed the expression of both *CYP19a1* and *HSD17b1* in cultures of granulosa cells, the overexpression of *FABP6* upregulated the *CYP19a1* gene, which is an estrogen synthesis-related gene. Together with our previous reports that *FABP6* is distributed in granulosa and luteal cells of rat ovaries [33–36], it seems quite probable that FXR-*FABP6* is related to steroidogenesis in granulosa cells, especially in estrogen biosynthesis. *FABP6* is an intracellular protein expressed in the distal ileum and plays a role in transcellular shuttling of bile acids [9–14]. Although the function of *FABP6* is not fully elucidated, even in enterohepatic tissues, it may be possible that *FABP6* has a role in transcellular shuttling of sex hormones in the ovary, as previous studies have demonstrated that *FABP6* is involved in intracellular transport of bile acids in enterocytes [14, 37, 38]. In *FABP6*-deficient mice [39], the ovulation rate after superovulatory treatment was markedly decreased compared to that in wild-type mice, which suggests that *FABP6* is involved in fertility via a function in granulosa cells.

In conclusion, the present study showed evidence for the existence of FXR signaling in ovarian granulosa cells. In addition, reproduction and metabolism are deeply related to each other; metabolic syndrome induces dysfunction of the ovary, such as menstrual abnormalities and ovulation disorder via an association with insulin resistance. FXR is a major regulatory factor for bile acid metabolism in enterohepatic tissues, and its deficiency results in abnormalities in glucose homeo-

stasis as well as in insulin resistance. In addition, intestine-specific FXR activation corrects numerous obesity-related defects, enhances glucose tolerance, and lowers hepatic glucose production, indicating that these physiologic changes are dependent on FXR expression [40]. Therefore, besides the action of FXR signaling in granulosa cells revealed in the present study, FXR signaling may have multiple functions in ovarian events. These findings suggest that potential new therapeutic targets in ovarian-related diseases may be developed by investigating ovarian FXR signaling.

**Conflic of interests:** The authors declare that there is no conflict of interest that could be perceived as prejudicing the impartiality of the research reported.

### Acknowledgements

The authors thank Drs S Iseki, K Morohaku, Y Takagi, and K Hamano for their helpful discussions.

This work was supported by Grant-in-Aid for Scientific Research (C) (grant number 18K05940); the Yamaguchi Educational and Scholarship Foundation (grant number H29-14); and by the Japan Association for Livestock New Technology (grant number H29-9) to IT.

### References

1. Adhikari D, Liu K. Molecular mechanisms underlying the activation of mammalian primordial follicles. *Endocr Rev* 2009; **30**: 438–464. [Medline] [CrossRef]
2. Nagy RA, van Montfoort AP, Dikkers A, van Echten-Arends J, Homminga I, Land JA, Hoek A, Tietge UJ. Presence of bile acids in human follicular fluid and their relation with embryo development in modified natural cycle IVF. *Hum Reprod* 2015; **30**: 1102–1109. [Medline] [CrossRef]
3. Sánchez-Guijo A, Blaschka C, Hartmann MF, Wrenzycki C, Wudy SA. Profiling of bile acids in bovine follicular fluid by fused-core-LC-MS/MS. *J Steroid Biochem Mol Biol* 2016; **162**: 117–125. [Medline] [CrossRef]
4. Sanchez R, Schuermann Y, Gagnon-Duval L, Baldassarre H, Murphy BD, Gevry N, Agellon LB, Bordignon V, Duggavathi R. Differential abundance of IGF1, bile acids, and the genes involved in their signaling in the dominant follicle microenvironment of lactating cows and nulliparous heifers. *Theriogenology* 2014; **81**: 771–779. [Medline] [CrossRef]
5. Smith LP, Nierstenhoefer M, Yoo SW, Penzias AS, Tobiasch E, Usheva A. The bile acid synthesis pathway is present and functional in the human ovary. *PLoS One* 2009; **4**: e7333. [Medline] [CrossRef]
6. Chen F, Ma L, Dawson PA, Sinal CJ, Schayek E, Gonzalez FJ, Breslow J, Ananthanarayanan M, Shneider BL. Liver receptor homologue-1 mediates species- and cell line-specific bile acid-dependent negative feedback regulation of the apical sodium-dependent bile acid transporter. *J Biol Chem* 2003; **278**: 19909–19916. [Medline] [CrossRef]
7. Goodwin B, Jones SA, Price RR, Watson MA, McKee DD, Moore LB, Galardi C, Wilson JG, Lewis MC, Roth ME, Maloney PR, Willson TM, Kliewer SA. A regulatory cascade of the nuclear receptors FXR, SHP-1, and LXR-1 represses bile acid biosynthesis. *Mol Cell* 2000; **6**: 517–526. [Medline] [CrossRef]
8. Lu TT, Makishima M, Repa JJ, Schoonjans K, Kerr TA, Auwerx J, Mangelsdorf DJ. Molecular basis for feedback regulation of bile acid synthesis by nuclear receptors. *Mol Cell* 2000; **6**: 507–515. [Medline] [CrossRef]
9. Coppola CP, Gosche JR, Arrese M, Ancowitz B, Madsen J, Vanderhoof J, Shneider BL. Molecular analysis of the adaptive response of intestinal bile acid transport after ileal resection in the rat. *Gastroenterology* 1998; **115**: 1172–1178. [Medline] [CrossRef]
10. Gong YZ, Everett ET, Schwartz DA, Norris JS, Wilson FA. Molecular cloning, tissue distribution, and expression of a 14-kDa bile acid-binding protein from rat ileal cytosol. *Proc Natl Acad Sci USA* 1994; **91**: 4741–4745. [Medline] [CrossRef]
11. Kramer W, Girbig F, Gutjahr U, Kowalewski S, Jouvenal K, Müller G, Tripiet D, Wess G. Intestinal bile acid absorption. Na(+)-dependent bile acid transport activity in rabbit small intestine correlates with the coexpression of an integral 93-kDa and a peripheral 14-kDa bile acid-binding membrane protein along the duodenum-ileum axis. *J Biol*



- Chem* 1993; **268**: 18035–18046. [Medline]
12. **Wong MH, Oelkers P, Craddock AL, Dawson PA.** Expression cloning and characterization of the hamster ileal sodium-dependent bile acid transporter. *J Biol Chem* 1994; **269**: 1340–1347. [Medline]
  13. **Fujita M, Fujii H, Kanda T, Sato E, Hatakeyama K, Ono T.** Molecular cloning, expression, and characterization of a human intestinal 15-kDa protein. *Eur J Biochem* 1995; **233**: 406–413. [Medline] [CrossRef]
  14. **Nakahara M, Furuya N, Takagaki K, Sugaya T, Hirota K, Fukamizu A, Kanda T, Fujii H, Sato R.** Ileal bile acid-binding protein, functionally associated with the farnesoid X receptor or the ileal bile acid transporter, regulates bile acid activity in the small intestine. *J Biol Chem* 2005; **280**: 42283–42289. [Medline] [CrossRef]
  15. **Cho SW, An JH, Park H, Yang JY, Choi HJ, Kim SW, Park YJ, Kim SY, Yim M, Baek WY, Kim JE, Shin CS.** Positive regulation of osteogenesis by bile acid through FXR. *J Bone Miner Res* 2013; **28**: 2109–2121. [Medline] [CrossRef]
  16. **Id Boufker H, Lagneaux L, Fayyad-Kazan H, Badran B, Najar M, Wiedig M, Ghanem G, Laurent G, Body JJ, Journé F.** Role of farnesoid X receptor (FXR) in the process of differentiation of bone marrow stromal cells into osteoblasts. *Bone* 2011; **49**: 1219–1231. [Medline] [CrossRef]
  17. **Huang C, Wang J, Hu W, Wang C, Lu X, Tong L, Wu F, Zhang W.** Identification of functional farnesoid X receptors in brain neurons. *FEBS Lett* 2016; **590**: 3233–3242. [Medline] [CrossRef]
  18. **Pu J, Yuan A, Shan P, Gao E, Wang X, Wang Y, Lau WB, Koch W, Ma XL, He B.** Cardiomyocyte-expressed farnesoid-X-receptor is a novel apoptosis mediator and contributes to myocardial ischaemia/reperfusion injury. *Eur Heart J* 2013; **34**: 1834–1845. [Medline] [CrossRef]
  19. **Zhang R, Ran HH, Zhang YX, Liu P, Lu CY, Xu Q, Huang Y.** Farnesoid X receptor regulates vascular reactivity through nitric oxide mechanism. *J Physiol Pharmacol* 2012; **63**: 367–372. [Medline]
  20. **Anaya-Hernández A, Méndez-Tepepa M, Hernández-Aragón LG, Pacheco P, Martínez-Gómez M, Castellán F, Cuevas E.** Farnesoid X receptor immunolocalization in reproductive tissues of adult female rabbits. *Acta Histochem* 2014; **116**: 1068–1074. [Medline] [CrossRef]
  21. **Catalano S, Malivindi R, Giordano C, Gu G, Panza S, Bonfiglio D, Lanzino M, Sisci D, Panno ML, Andò S.** Farnesoid X receptor, through the binding with steroidogenic factor 1-responsive element, inhibits aromatase expression in tumor Leydig cells. *J Biol Chem* 2010; **285**: 5581–5593. [Medline] [CrossRef]
  22. **Kaeding J, Bouchaert E, Bélanger J, Caron P, Chouinard S, Verreault M, Larouche O, Pelletier G, Staelens B, Bélanger A, Barbier O.** Activators of the farnesoid X receptor negatively regulate androgen glucuronidation in human prostate cancer LNCAP cells. *Biochem J* 2008; **410**: 245–253. [Medline] [CrossRef]
  23. **Gray MA, Squires EJ.** Effects of nuclear receptor transactivation on steroid hormone synthesis and gene expression in porcine Leydig cells. *J Steroid Biochem Mol Biol* 2013; **133**: 93–100. [Medline] [CrossRef]
  24. **Watanabe T, Nishimura K, Hosaka YZ, Shimosato T, Yonekura S, Suzuki D, Takemoto C, Monir MM, Hiramatsu K.** Histological analysis of glucagon-like peptide-1 receptor expression in chicken pancreas. *Cell Tissue Res* 2014; **357**: 55–61. [Medline] [CrossRef]
  25. **Vaquero J, Monte MJ, Dominguez M, Muntané J, Marin JJ.** Differential activation of the human farnesoid X receptor depends on the pattern of expressed isoforms and the bile acid pool composition. *Biochem Pharmacol* 2013; **86**: 926–939. [Medline] [CrossRef]
  26. **Forman BM, Goode E, Chen J, Oro AE, Bradley DJ, Perlmann T, Noonan DJ, Burka LT, McMorris T, Lamph WW, Evans RM, Weinberger C.** Identification of a nuclear receptor that is activated by farnesol metabolites. *Cell* 1995; **81**: 687–693. [Medline] [CrossRef]
  27. **Abu-Hayyeh S, Papacleovoulou G, Lövgren-Sandblom A, Tahir M, Oduwole O, Jamaludin NA, Ravat S, Nikolova V, Chambers J, Selden C, Rees M, Marshall HU, Parker MG, Williamson C.** Intrahepatic cholestasis of pregnancy levels of sulfated progesterone metabolites inhibit farnesoid X receptor resulting in a cholestatic phenotype. *Hepatology* 2013; **57**: 716–726. [Medline] [CrossRef]
  28. **Wang S, Lai K, Moy FJ, Bhat A, Hartman HB, Evans MJ.** The nuclear hormone receptor farnesoid X receptor (FXR) is activated by androsterone. *Endocrinology* 2006; **147**: 4025–4033. [Medline] [CrossRef]
  29. **Fayard E, Auwerx J, Schoonjans K.** LRH-1: an orphan nuclear receptor involved in development, metabolism and steroidogenesis. *Trends Cell Biol* 2004; **14**: 250–260. [Medline] [CrossRef]
  30. **Zhao H, Li Z, Cooney AJ, Lan ZJ.** Orphan nuclear receptor function in the ovary. *Front Biosci* 2007; **12**: 3398–3405. [Medline] [CrossRef]
  31. **Duggavathi R, Volle DH, Matakic C, Antal MC, Messaddeq N, Auwerx J, Murphy BD, Schoonjans K.** Liver receptor homolog 1 is essential for ovulation. *Genes Dev* 2008; **22**: 1871–1876. [Medline] [CrossRef]
  32. **Zhang C, Large MJ, Duggavathi R, DeMayo FJ, Lydon JP, Schoonjans K, Kovanci E, Murphy BD.** Liver receptor homolog-1 is essential for pregnancy. *Nat Med* 2013; **19**: 1061–1066. [Medline] [CrossRef]
  33. **Iseki S, Amano O, Fujii H, Kanda T, Ono T.** Immunohistochemical localization of two types of fatty acid-binding proteins in rat ovaries during postnatal development and in immature rat ovaries treated with gonadotropins. *Anat Rec* 1995; **241**: 235–243. [Medline] [CrossRef]
  34. **Iseki S, Amano O, Kanda T, Fujii H, Ono T.** Expression and localization of intestinal 15 kDa protein in the rat. *Mol Cell Biochem* 1993; **123**: 113–120. [Medline] [CrossRef]
  35. **Fujii H, Nomura M, Kanda T, Amano O, Iseki S, Hatakeyama K, Ono T.** Cloning of a cDNA encoding rat intestinal 15 kDa protein and its tissue distribution. *Biochem Biophys Res Commun* 1993; **190**: 175–180. [Medline] [CrossRef]
  36. **Sato E, Fujii H, Fujita M, Kanda T, Iseki S, Hatakeyama K, Tanaka T, Ono T.** Tissue-specific regulation of the expression of rat intestinal bile acid-binding protein. *FEBS Lett* 1995; **374**: 184–186. [Medline] [CrossRef]
  37. **Praslickova D, Torchia EC, Sugiyama MG, Magrane EJ, Zwicker BL, Kolodzieyski L, Agellon LB.** The ileal lipid binding protein is required for efficient absorption and transport of bile acids in the distal portion of the murine small intestine. *PLoS One* 2012; **7**: e50810. [Medline] [CrossRef]
  38. **Zwicker BL, Agellon LB.** Transport and biological activities of bile acids. *Int J Biochem Cell Biol* 2013; **45**: 1389–1398. [Medline] [CrossRef]
  39. **Duggavathi R, Siddappa D, Schuermann Y, Pansera M, Menard IJ, Praslickova D, Agellon LB.** The fatty acid binding protein 6 gene (Fabp6) is expressed in murine granulosa cells and is involved in ovulatory response to superstimulation. *J Reprod Dev* 2015; **61**: 237–240. [Medline] [CrossRef]
  40. **Fang S, Suh JM, Reilly SM, Yu E, Osborn O, Lackey D, Yoshihara E, Perino A, Jacinto S, Lukasheva Y, Atkins AR, Khvat A, Schnabl B, Yu RT, Brenner DA, Coulter S, Liddle C, Schoonjans K, Olefsky JM, Saltiel AR, Downes M, Evans RM.** Intestinal FXR agonism promotes adipose tissue browning and reduces obesity and insulin resistance. *Nat Med* 2015; **21**: 159–165. [Medline] [CrossRef]